Received: 30 December 2020 | Revised: 18 May 2021 | Accepted: 23 May 2021

DOI: 10.1111/jzs.12505

JOURNAL OF ZOOLOGICAL SYSTEMATICS AND EVOLUTIONARY RESEARCH — WILEY

ORIGINAL ARTICLE

Intraspecific morphological variation in the shieldtail snake *Rhinophis philippinus* (Serpentes: Uropeltidae), with particular reference to tail-shield and cranial 3D geometric morphometrics

Lucy C. Huntley[1,2] | David J. Gower[1] | Filipa L. Sampaio[1,2] | Ellen S. Collins[1,3] | Anjali Goswami[1] | Anne-Claire Fabre[1]

[1]Department of Life Sciences, The Natural History Museum, London, UK

[2]Department of Genetics, Evolution and Environment, University College London, London, UK

[3]Department of Animal and Plant Sciences, University of Sheffield, Sheffield, UK

Correspondence
Lucy C. Huntley and Anne-Claire Fabre, Department of Life Sciences, The Natural History Museum, London SW7 5BD, UK.
Emails: lucy.huntley.19@ucl.ac.uk (LCH); a.fabre@nhm.ac.uk (A-CF)

Funding information
Systematics Research Fund grant from the UK's Systematics Association and the Linnean Society of London; UCL Bogue Fellowship; H2020 European Research Council, Grant/Award Number: STG-2014–637171; Natural Environment Research Council, Grant/Award Number: NE/ L002485/1

Abstract

The Uropeltidae, a family of small, fossorial snakes endemic to south Asia, are characterized by highly modified head and tail morphology. Their secretive nature has led to a dearth of research regarding intraspecific variation in morphology and tail function. Linear morphometrics of external size and shape and scale counts were combined with 3D geometric morphometric analysis of high-resolution computed tomography scans of crania and bony tail-shields to assess intraspecific morphological variation in 35 specimens of *Rhinophis philippinus*. Cranial and tail-shield shape differences are slight and subtle, though both exhibited significant allometry. Significant sexual dimorphism was found only in numbers of ventral scales, numbers of subcaudal scales, and tail length. There is no evidence of sexual dimorphism in head, cranial or tail-shield shape and size. It is hypothesized that strong functional constraints, induced by head-first burrowing in *R. philippinus*, have led to strong stabilizing selection in head and cranial shape, with functional constraints outweighing any influence of sexual selection. Lack of tail-shield sexual dimorphism (despite strong tail length dimorphism) suggests a common function in both sexes, likely related to predator avoidance and defense.

KEYWORDS
allometry, fossorial, morphology, sexual dimorphism

RÉSUMÉ

Les Uropeltidae, une famille de petits serpents fouisseurs endémiques de l'Asie du Sud, sont caractérisés par une morphologie de la tête et de la queue très modifiée. Leur mode de vie difficile à étudier est à l'origine du manque de connaissances concernant la variation intraspécifique de la morphologie et de la fonction de leur queue. Afin de mieux

Contributing authors: David J. Gower (d.gower@nhm.ac.uk), Filipa L. Sampaio (f.sampaio@nhm.ac.uk), Ellen S. Collins (escollins1@sheffield.ac.uk), Anjali Goswami (a.goswami@nhm.ac.uk)

de mieux comprendre la variation morphologique du crâne et des boucliers caudaux osseux de ces espèces, nous avons réalisé une étude intraspécifique sur 35 spécimens de *Rhinophis philippinus*. Pour cela, nous avons utilisé des approches de morphométrie linéaire de la taille, de la forme externe ainsi que le nombre d'écailles combinées à des analyses de morphométrie géométrique 3D. Les différences de forme du crâne et du bouclier caudal sont subtiles, bien que les deux présentent une allométrie significative. Un dimorphisme sexuel significatif a été trouvé seulement pour le nombre d'écailles ventrales, le nombre d'écailles subcaudales et la longueur de la queue. Les résultats ne montrent pas de dimorphisme sexuel dans la forme et la taille de la tête, du crâne ou du bouclier caudal. Ces résultats semblent soutenir les hypothèses qui suggèrent que de fortes contraintes fonctionnelles, induites par le fouissage la tête la première chez *R. philippinus*, ont conduit à une forte sélection stabilisatrice de la forme de la tête et du crâne, les contraintes fonctionnelles l'emportant sur toute influence de la sélection sexuelle. L'absence de dimorphisme sexuel du bouclier caudal (malgré un fort dimorphisme de la longueur de la queue) suggère une fonction commune aux deux sexes, probablement liée à l'évitement des prédateurs et à la défense.

1 | INTRODUCTION

Uropeltidae ("shieldtails") is a family of fossorial snakes endemic to Sri Lanka and peninsular India (Pyron et al., 2016). The approximately 60 extant species (Uetz et al., 2020) are characterized by small sizes (typically <50 cm total length), cylindrical bodies, small and often pointed heads, and in most cases substantially modified tail structures ("shields"). In the most elaborate condition, the last few vertebrae are fused and terminate in a bony structure that underlies one or more specialized scales, such that there can be both an external shield and internal, bony shield (Baumeister, 1908; Gans, 1976). The external shield varies substantially among genera and species, from a single, large, domed, or conical scale in *Rhinophis* to a convex or flat posterodorsal surface formed by multiple, multi-keeled scales in *Uropeltis*. The external shield has been used extensively by systematists (Pyron et al., 2016) but the internal structure has been little studied. Uropeltids are generally poorly known. They have a somewhat confusing and incompletely resolved taxonomy (Comeaux et al., 2010; Gower et al., 2008; Pyron et al., 2016) that makes many of them difficult to identify, especially in the field. Combined with their typically hidden, mostly soil-dwelling existence, this has resulted in a dearth of natural history information, particularly from studies in life. Thus, we know very little of their locomotion, diets, populations, and inter- and intraspecific interactions.

Improved knowledge of uropeltids is informative beyond the group and might have implications for understanding the early evolution of snakes. Phylogenetically, uropeltids lie outside a clade comprising the vast majority of all other extant snakes and are possibly closely related to the clade comprising Pythonoidea, Booidea, and Bolyeriidae (Burbrink et al., 2020). Currently, the orthodox view of snake origins is that at least some snake traits were acquired as adaptations to fossoriality (Da Silva et al., 2018; Miralles et al., 2018). Whether or not fossoriality in uropeltids is retention of an ancestral snake feature, shieldtails are an entirely fossorial, speciose, and phenotypically diverse radiation, and so offer great potential to understand evolutionary responses of snakes to life in soil.

Beyond foundational studies of single taxa (Baumeister, 1908) or broader overviews in the context of snake diversity (Cundall & Irish, 2008; Underwood, 1967), previous research on uropeltid osteology has mainly focused on interspecific cranial variation, and on using this information to infer phylogeny and test classifications (Olori & Bell, 2012; Pyron et al., 2016; Rieppel & Zaher, 2002). No studies to date have explicitly investigated intraspecific morphological variation in uropeltids in relation to sexual dimorphism and/or function. However, investigating intraspecific variation is important because it provides insights into how morphological, functional, and ecological traits vary within populations, which is vital for systematic and evolutionary research (Fabre et al., 2014; Fabre et al., 2014; Kaliontzopoulou et al., 2007; Rivas & Burghardt, 2001; Shine, 1994). Furthermore, as selection occurred at the level of the population, it can be informative concerning the evolutionary processes shaping organismal variation and can also aid in the identification of new species.

Sexual dimorphism has emerged as an important aspect of uropeltid biology that is open to investigation using static museum specimens, and which has implications for understanding other aspects of uropeltid natural history. Many, but not all, uropeltid species are sexually dimorphic in tail length and numbers of subcaudal scales (Boulenger, 1893; Constable, 1949; Cyriac et al., 2020; Gower, 2020; Gower et al., 2016; Guibé, 1948; Jins et al., 2018; Wall, 1919, 1921), and some are also sexually dimorphic in numbers of ventral scales (which correspond to the number of pre-caudal vertebrae (Alexander & Gans, 1966) and in the prominence of longitudinal ridges (keels) on scales under the tail and posterior end of the body (Cyriac et al., 2020; Jins et al., 2018). Greater appreciation and analysis of these widespread sexual dimorphisms have had a substantial positive impact on taxonomic revision of uropeltids, and the

recognition and description of several new species (Jins et al., 2018; Sampaio et al., 2020).

As yet, there are no reports of sexual dimorphism in uropeltid heads. Although there is some evidence of sexual dimorphism in the flattened, multi-scaled tail-shields of *Uropeltis*, with relatively longer, narrower shields in males (Jins et al., 2018), there have been no reports thus far of sexual dimorphism in the often large, domed tail-shields of *Rhinophis*. Uropeltid heads might be expected to not be dimorphic given potentially strong constraints imposed by head-first burrowing (Delêtre & Measey, 2004; Heideman et al., 2008), assuming that males and females are similarly fossorial—something that is unknown. However, Cyriac and Kodandaramaiah (2020) reported notable variation in interspecific head shape in some species of *Uropeltis*, suggesting that investigations of intraspecific variation would also be worthwhile. Uropeltid tail-shields are mysterious in their origin and function. Although the current dominant view is that uropeltid tail-shields play a role in cephalic mimicry to divert attention of predators away from the typically small, inconspicuous head while to some extent simultaneously protecting the tail (Cyriac & Kodandaramaiah, 2019; Gans, 1976, 1986b), other functions have been proposed, such as blocking burrows (Gans, 1976; Gans & Baic, 1977) and in locomotion (Clark, 1966). Tail-shield dimorphism might be expected if this structure is involved in sexual selection or is involved in some role in which male and female ecology or behavior differed. Alternatively, dimorphism in this structure may simply be a by-product of sexual size dimorphism, with males typically having longer tails than their female counterparts.

Here, we report a detailed investigation of shape variation and sexual dimorphism in a sample of the Sri Lankan uropeltid *Rhinophis philippinus* (Cuvier & Latreille, 1829) (Figure 1). We use both linear and geometric morphometrics to investigate whether cranial and tail-shield shape covaries, whether variations are influenced by size through allometry and if these structures exhibit sexual dimorphism and/or functional signal in shape or size. If any sexual dimorphism is observed, we expect to observe differences in size and/or morphology between males and females (Fitch, 1981). If the tail and/or the head perform a similar function in males and females, we expect no shape differences between the sexes.

2 | MATERIALS AND METHODS

2.1 | Specimens and external morphology

Morphometric data were collected for 35 specimens of *R. philippinus*, comprising 16 males, 18 females, and one of unknown sex (Table 1). All specimens are spirit-preserved and stored in the permanent collections of the Natural History Museum, London, UK (BNMH) and the Muséum National d'Histoire Naturelle, Paris, France (MNHN). Tail length was used to infer sex of all specimens given that it was found to be strongly dimorphic (see below). Sex was determined for a few specimens by examination of the urogenital system via small incisions—as in the many other species of *Rhinophis* with dimorphic tail length (Cyriac et al., 2020; Gower, 2020), longer and shorter tails were always found in males and females, respectively. Eight linear measurements were taken using dial calipers to the nearest 0.1mm: tail length, head length (snout tip to posterior of fourth supralabial), head width (at posterior ends of fourth supralabials), midbody width, tail-shield middorsal length (shortest distance between posterior tip and anterodorsal midline limit of shield), tail-shield midventral length (shortest distance between posterior tip and anteroventral midline limit of shield), tail-shield height at base (shortest distance between anterodorsal and anteroventral midline limits of shield), tail-shield width at base (maximum transverse width of base of shield). Total length was measured by a ruler to the nearest 1 mm, and snout-vent length was determined by subtracting tail length from body length. Counts were taken of the total ventral scales (following Gower and Ablett (2006)), mean of left and right subcaudal scales, unpaired or fused subcaudal scales, and scales around the perimeter of the shield base.

2.2 | Imaging cranial and tail-shield osteology

The heads and tails of all specimens were scanned using a Nikon Metrology X-Tek HMX ST 225 micro-CT scanner (BNMH specimens) and a v|tome|x L 240–180" model from GE Sensing & Inspection Technologies phoenix x|ray scanner (MNHN specimen).

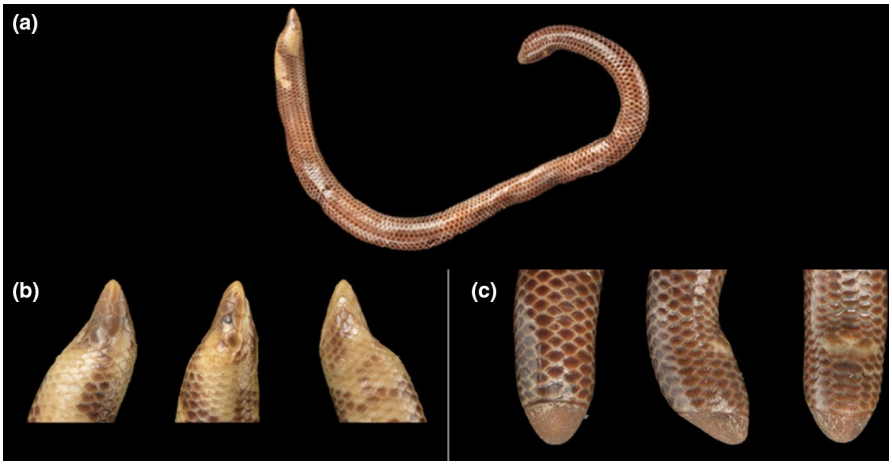

FIGURE 1 *Rhinophis philippinus* specimen BMNH 1946.1.16.9, showing the whole specimen (a) and the head (b) and tail (c) in dorsal, lateral, and ventral views. Total length of the specimen is 155 mm. Photographs by Kevin Webb (NHM, London)

TABLE 1 External metric (in mm) and meristic character data for 35 specimens of *Rhinophis philippinus*

Specimen & Collection	Sex	TL	tL	SVL	HL	HW	Mb W	SLd	SLv	SBH	SBW	Ven	SC	SCu	PS
1964.1670 (BMNH)	f	180	4.7	175.3	4.8	3.2	5.3	4.9	2.5	4.5	4.4	176	3.0	0	13
1964.1671 (BMNH)	f	148	5.1	142.9	5.1	3.7	6.3	5.3	2.2	5.0	4.6	175	4.0	3	13
1964.1672 (BMNH)	m	158	6.2	151.8	4.9	3.1	5.0	4.5	1.9	4.2	4.1	166	6.0	1	14
1964.1673 (BMNH)	f	178	4.7	173.3	5.2	3.8	5.7	5.3	2.2	5.1	4.8	174	4.0	2	14
1964.1674 (BMNH)	m	121	5.8	115.2	4.8	3.8	5.7	5.0	2.2	4.7	4.2	161	6.0	3	14
1964.1675 (BMNH)	f	132	3.4	128.6	4.3	3.2	3.9	4.4	1.7	4.3	3.8	172	3.0	2	12
1964.1676 (BMNH)	m	131	6.4	124.6	4.6	3.3	5.0	4.3	2.0	4.2	3.9	161	5.5	1	13
1964.1677 (BMNH)	m	118	4.7	113.3	4.4	3.1	3.8	4.1	1.5	3.9	3.5	161	5.0	2	11
1964.1690 (BMNH)	f	198	5.3	192.7	5.1	3.4	5.3	5.5	2.1	5.2	4.8	176	4.0	3	12
1964.1691 (BMNH)	m	167	6.0	161.0	4.7	3.3	5.0	5.4	2.2	5.1	4.6	164	6.0	4	14
1964.1692 (BMNH)	f	137	3.7	133.3	4.5	3.0	4.2	4.3	1.7	4.1	3.7	177	3.0	2	12
1964.1693 (BMNH)	m	172	6.5	165.5	5.2	3.5	5.7	5.2	2.2	4.6	4.2	163	5.0	2	11
1964.1694 (BMNH)	f	211	3.7	207.3	5.8	3.7	5.4	6.2	2.6	5.0	5.6	179	3.0	1	12
1964.1695 (BMNH)	m	136	4.5	131.5	4.5	3.0	5.2	4.8	2.1	4.3	4.1	163	5.0	1	12
1964.1696 (BMNH)	m	165	6.4	158.6	4.8	3.0	4.6	5.0	2.2	4.7	4.0	161	5.0	4	12
1964.1697 (BMNH)	m	131	5.6	125.4	4.5	3.2	4.5	4.5	1.8	4.3	3.7	162	5.5	3	11
1964.1698 (BMNH)	f	105	3.1	101.9	4.0	2.5	3.4	3.7	1.5	3.7	3.2	170	3.0	2	11
1964.1699 (BMNH)	m	105	5.4	99.6	4.0	2.9	3.0	4.2	1.6	3.7	3.1	166	6.0	4	13
1964.1700 (BMNH)	f	150	4.0	146	4.4	2.7	3.8	4.9	2.0	4.9	4.0	174	3.0	1	12
1964.1701 (BMNH)	f	91	2.6	88.4	4.0	3.0	3.7	3.1	1.0	3.1	3.0	169	4.0	3	12
1964.1702 (BMNH)	m	134	5.7	128.3	4.6	3.3	4.5	4.6	2.1	4.4	4.0	163	5.0	2	12
1964.1703 (BMNH)	f	123	3.6	119.4	4.2	3.2	3.8	4.0	1.5	3.5	3.4	177	3.5	1	13
1964.1704 (BMNH)	m	161	6.6	154.4	4.9	3.6	4.8	5.1	2.2	4.8	4.1	166	5.0	4	13
1964.1705 (BMNH)	u	115	3.9	111.1	4.1	2.5	3.8	3.5	1.3	3.5	3.0	177	6.0	1	13
1964.1706 (BMNH)	f	84	2.9	81.1	3.8	2.6	2.7	3.1	1.1	3.0	2.7	176	4.0	3	13
1964.1707 (BMNH)	f	187	5.1	181.9	5.1	3.5	5.6	5.6	2.3	5.2	4.7	170	4.0	3	12
1964.1708 (BMNH)	m	142	4.9	137.1	4.6	3.0	4.3	4.6	2.1	4.4	4.1	160	5.0	3	12
1964.1709 (BMNH)	f	82	2.4	79.6	3.8	2.3	2.6	3.1	1.2	2.8	2.5	173	3.0	1	12
1964.1710 (BMNH)	f	125	3.3	121.7	4.3	2.7	3.7	4.2	1.6	4.0	3.7	175	3.0	1	12
1964.1711 (BMNH)	f	100	3.0	97.0	3.8	2.6	3.5	3.2	1.2	3.0	2.8	171	4.0	3	11
1964.1712 (BMNH)	m	86	4.5	81.5	3.8	2.9	3.4	3.3	1.2	3.3	3.0	163	6.0	4.0	11
1968.5170 (BMNH)	f	186	4.4	181.6	4.9	3.6	7.2	5.0	1.9	4.9	4.8	169	3.5	0	14
1946.1.16.99 (BMNH)	m	155	6.0	149.0	4.9	3.8	5.2	5.1	1.9	5.0	4.5	157	6.0	5	13
6994 (MNHN)	f	259	6.4	252.6	6.5	4.4	7.4	6.3	2.8	6.1	5.8	173	3.5	1	11
98.5.3.11 (BMNH)	m	153	6.2	146.8	5.1	4.6	5.2	5.0	1.9	4.8	4.3	157	5.5	0	13

Note: Specimens are in the collections of the Natural History Museum, London (BMNH prefix) and Muséum National d'Histoire Naturelle, Paris (MNHN). Character abbreviations as follows: HL, head length, snout tip to back of fourth supralabial; HW, head width at back of fourth supralabials; Mb W, midbody width; PS, number of scales around perimeter of base of tail-shield; SBH, height of tail-shield base; SBW, width of tail-shield base; SC, mean of left and right numbers of subcaudal scales; SCu, total number of unpaired ["fused"] subcaudal scales; SLd, middorsal length of tail-shield; SLv, midventral length of tail-shield; SVL, snout-vent length; tL, tail length; TL, total length; Ven, number of ventral scales.

Reconstructed scan data were digitally segmented using Avizo Lite v.9.3 (FEI). These meshes were imported into Geomagic Wrap (3D Systems) and osteologically distinct, extraneous components such as vertebrae, quadrates, and lower mandibles were digitally removed. The outer surface of the bony tail-shields has many pits and holes that were filled manually using Geomagic in order to facilitate shape quantification procedures. Meshes were decimated to less than one million faces to reduce computational demand when landmarking, but still maintain enough detail to pick up any fine intraspecific variation. Two of the crania (BMNH 1964.1676 and BMNH

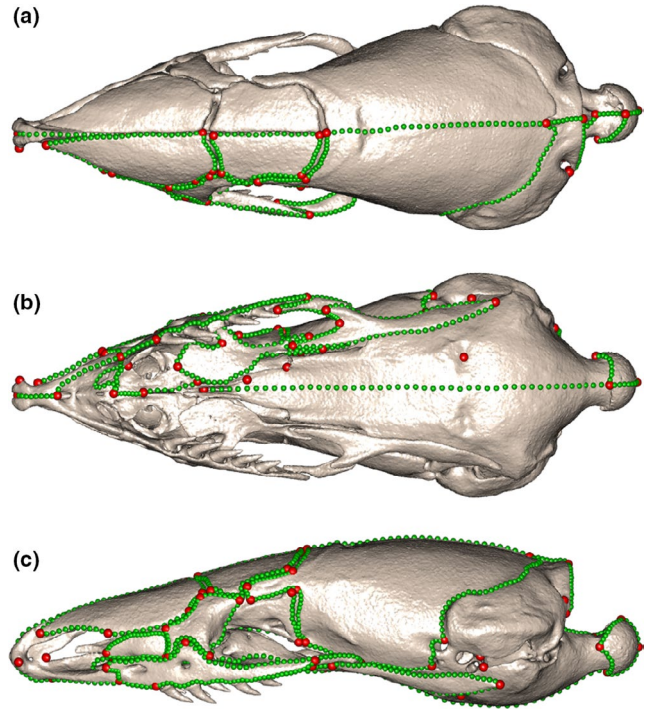

FIGURE 2 Images of the cranium of *Rhinophis philippinus* specimen BMNH 1964.1672 with landmarks (red) and curve semilandmarks (green), shown in dorsal (a), ventral (b), and lateral (c) views

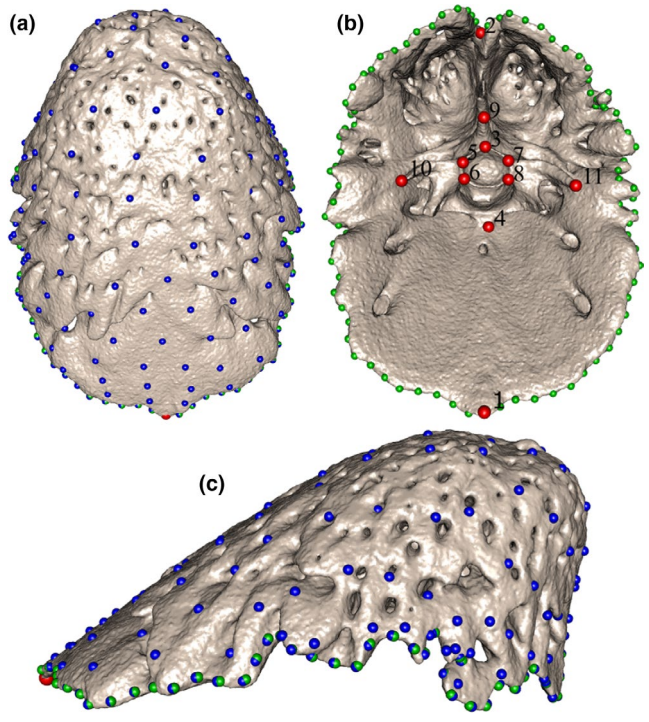

FIGURE 3 Images of the bony tail-shield of *Rhinophis philippinus* specimen BMNH 1964.1676 with landmarks (red), curve semilandmarks (green), and surface semilandmarks (blue), shown in dorsal (a), ventral (b), and lateral (c) views. The landmarks on (b) are labeled corresponding to Table S3. For all views, posterior is to the top

98.5.3.11) were mirrored using the "mirror" function because their left sides were damaged. Subsequent analyses were carried out on the left side of all crania. Two of the crania (BMNH 1964.1674 and BMNH 1968.5170) were too broken to be landmarked, and so were removed from the cranial dataset. All meshes used in this study are availble on Phenome10K (http://www.phenome10k.org/).

2.3 | Geometric morphometrics

The complexity of the morphology of the cranium and irregular, monolithic nature of the tail-shield would be greatly underrepresented by linear measurements alone. Geometric morphometrics uses landmarks to pinpoint homologous points throughout these complex shapes to describe the geometry of the object. Landmarks were generated on the surface of the reconstructed meshes using Checkpoint (Stratovan).

2.3.1 | Crania

Sixty-six Type I and Type II landmarks (Bookstein, 1992) were defined (Table S1) and placed on the left side of each cranial mesh (Figure 2). These landmarks served as homologous points, between which curve semilandmarks could be placed to delineate bones and regions of the crania. Here, we used a combined landmark and sliding semilandmark procedure to fully capture the complexities of the whole overall cranial shape. Fifty-six curves were placed on each cranial mesh (Table S2, Figure 2), and these were resampled such that each specimen had 818 curve semilandmark points in total. Curve semilandmarks were then slid using the "slider3d" function from the R package *Morpho* (Schlager, 2017) to minimize bending energy. This generated a dataset of homologous points that could be compared across the specimens.

2.3.2 | Bony tail-shields

The external tail-shield of *Rhinophis* spp. is underlain by a closely matching osteological structure fused to the last few caudal vertebrae and referred to here as the bony tail-shield. Type II landmarks were placed at the anterodorsomedial and posteroventromedial ends of the bony shield, and on nine homologous points of the vertebrae fused to it, totaling 11 landmarks (Table S3, Figure 3b). These landmarks did not capture the overall shape of the bony shield, and so they were combined with sliding curve and surface semilandmarks. Two curves were used to delineate the bony shield, anchored by the two landmarks at the anterior and posterior ends (Figure 3). These were resampled so that each curve had 45 semilandmarks, a total of 90 curve semilandmarks per specimen. In order to capture the shape of the outer surface of the bony shield, a template was created to place surface semilandmarks onto all the specimens. One specimen (BMNH 1946.1.16.99), deemed to be among the

specimens closest to the average bony-shield shape, was selected and duplicated with the landmark and curve semilandmark scheme detailed above. A specimen template was used instead of a generic hemispherical structure because variation is likely to be fine for an intraspecific dataset. Surface semilandmarks were placed on the template in a grid formation, with 16 rows spanning the dorsal surface of the bony shield. The template was then projected onto the other 34 bony shields in a semi-automatic patching procedure using the *Morpho* package in RStudio (Figure 3). The projected semilandmarks were checked using the "checkLM" function in *Morpho* to ensure an even distribution of points on all specimens fully captured the shape.

The inner surface of several bony-shield meshes was removed to prevent the surface semilandmarks falling underneath the dorsal surface. An additional curve was temporarily placed along the midline of the dorsal surface on eight specimens in order to redistribute the surface semilandmarks more evenly. A new template with this extra curve was used to project the surface semilandmarks onto those eight specimens. The surface semilandmarks were each expanded along their normals to differing extents, ensuring an even distribution that covered the entire shield outer surface. A total of 127 surface semilandmarks were projected onto the outer surface of each bony shield. Those surface semilandmarks, as well as the curve semilandmarks, were then slid, minimizing bending energy, using the "slider3d" function in *Morpho*. This procedure allows surface and curve semilandmarks to be transformed into geometrically homologous landmarks in order to compare shapes (Parr et al., 2012). The homologous landmarks and sliding semilandmarks were then compared across specimens using traditional morphometric methods.

2.3.3 | Generalized Procrustes alignment

The landmarks and semilandmarks were mirrored onto the right side of the crania, using the function "mirrorfill" from the package *paleomorph* (Lucas & Goswami, 2017), to produce a bilateral configuration that would result in a better Procrustes alignment. A generalized Procrustes alignment (Rohlf & Slice, 1990) was then carried out on the crania and bony-shield datasets using the "gpagen" function from the *geomorph* package (Adams et al., 2020). This removed non-shape data from the dataset, including translation, rotation, and isometric size, and so allowed the shape of specimens to be compared accurately. Finally, the mirrored landmarks and semilandmarks were removed from the right side of the crania for further analyses.

2.4 | Statistical analyses

Outlier plots were initially produced to ensure landmarks were placed in the correct order across all specimens. These plots also indicated that the cranium of one specimen (MNHN 6994) is substantially larger than the other specimens, and one of the smallest specimens (BMNH 1964.1701: Figure S1) has a notably less well ossified and more irregularly shaped bony tail-shield. These specimens were removed from further analyses, excluding the regression and linear dimensions analyses.

2.4.1 | Assessing the impact of size on shape using regression

In order to assess the impact of size on cranial and bony-shield shape (allometry), a regression of the log-transformed centroid size on the shape data was performed, using the "procD.lm" function in the R package *geomorph*. To identify which aspects of shape vary with size, regression plots were produced with the associated minimum and maximum shapes. The effect of allometry was corrected for in subsequent analyses by using the residuals from this regression as shape data. Procrustes residuals of the regression can thus be used to conduct analyses with shape data, taking into account allometry effects (Klingenberg, 2016).

2.4.2 | Principal components analyses

Principal components analyses (PCAs) were performed on both the cranial and the bony-shield residual shape data using the "plotTangentSpace" function in *geomorph* to investigate the distribution of the specimens in morphological space, and to identify the main axes of shape variation. Eigen values were generated to quantify the percentage of shape variation explained by each PC axis.

2.4.3 | Two-block partial least squares

A two-block partial least squares (2B-PLS) analysis (Rohlf & Corti, 2000) was conducted to detect covariation between the shape of the crania and the tail-shields. A covariance matrix was generated, made up of two blocks that represented the Procrustes coordinates of the cranial shape and of the bony-shield shape. This matrix identified which variables within one block were most likely to predict the variables in the other block (Zelditch et al., 2004). These were then compared using the "pls2B" function in *Morpho*. This test generated a PLS correlation coefficient, *r-PLS*, which estimated the degree of covariation between the two structures. The test was repeated using the residual shape data corrected for allometry, to assess if the covariation was related to size rather than shape. The 2B-PLS analysis also generated axes along which the covariation between the two blocks could be visualized.

2.4.4 | Shape visualization

Visualization of the cranial and bony tail-shield shape at each axis extreme of the regression, PCA, and 2B-PLS analyses was carried out using the functions "tps3d" from the package *Morpho* and "shade3d"

from the package *rgl* (Adler et al., 2020). These functions perform a thin-plate spline deformation of the meshes, producing a 3D image of each extreme (Bookstein, 1989).

2.4.5 | Tests of sexual dimorphism

To assess the morphological differences depending on sex, univariate analyses of variance (ANOVAs) were run on the log-transformed external morphology linear measurements, using the "lm" function from the *stats* package (R Core Team, 2019), and Kruskal–Wallis tests were run on the scale count data using the "kruskal.test" function from the *stats* package. Log-transformed centroid size data and Procrustes residuals of the regression on shape data were used as inputs in the following analyses. A multivariate analysis of variance (MANOVA) and an ANOVA were used to test for shape and size differences, respectively, for crania and bony shields depending on sex, using the "procD.lm" function in the *geomorph* package (Adams et al., 2020). Finally, to test whether disparity of males and females differ, we used the "morphol.disparity" function in *geomorph* on both the crania and bony tail-shields (Zelditch et al., 2004), providing an estimate of Procrustes variance (Pv).

2.4.6 | Tests of correlation between centroid size and external morphology

To assess if the centroid size is a good proxy of body size, we performed correlation tests using the "cor.test" function from the *stats* package. Correlations were assessed between cranial centroid size and snout-vent length, cranial centroid size and tail length, bony tail-shield centroid size and snout-vent length, bony tail-shield centroid size and tail length, head length and cranial centroid size.

3 | RESULTS

3.1 | External morphology

Raw data are reported in Table 1. Results of the analyses performed on the external morphological measurements and counts show that the following measurements are not sexually dimorphic: snout-vent length (SVL; ANOVA: $F = 0.174$, $p = 0.679$; though note that the seven largest specimens are all female); head length (ANOVA: $F = 0.036$, $p = 0.851$), head width (ANOVA: $F = 1.206$, $p = 0.280$); midbody width (ANOVA: $F = 0.208$, $p = 0.651$); tail-shield middorsal length (ANOVA: $F = 0.421$, $p = 0.521$); tail-shield midventral length (ANOVA: $F = 0.976$, $p = 0.331$); tail-shield height at base (ANOVA: $F = 0.424$, $p = 0.520$); tail-shield width at base (ANOVA: $F = 0.017$, $p = 0.896$); total fused subcaudal scales (Kruskal–Wallis: $H = 3.786$, $p = 0.052$); total shield perimeter scales (Kruskal–Wallis: $H = 0.220$, $p = 0.639$).

In contrast, tail length is significantly dimorphic (ANOVA: $F = 27.81$, $p < 0.0001$), being longer in males than females. This dimorphism is still apparent when tail length is considered relative to size (SVL in this case: ANCOVA: $F = 91.91$, $p < 0.0001$). Numbers of ventral and mean of left and right numbers of subcaudal scales are also significantly sexually dimorphic (Kruskal–Wallis: $H = 24.818$, $p < 0.0001$ and $H = 25.621$, $p < 0.0001$, respectively). On average, females have more ventral scales (males: range = 157–166, average = 162.1; females: range = 169–179, average = 173.7) and fewer mean subcaudal scales (males: range = 5–6, average = 5.5; females: range = 3–4, average = 3.5).

3.2 | Cranial and bony tail-shield allometry

Regressions of $\log_{10}$-transformed centroid size against shape show that allometry has a significant effect on shape for both crania ($R^2 = 0.238$, $p = 0.0001$) and bony tail-shields ($R^2 = 0.151$, $p = 0.0001$).

The scatterplot of the regression of cranial $\log_{10}$-transformed centroid size against shape (Figure S2) shows a strong linear relationship with little scatter. Larger crania tend to have a relatively lower, less dorsally arched cranial cavity, a longer occipital condyle stalk, and a slightly posteriorly flared exoccipital arch (Figure S2). The lack of separate clustering of the two sexes provides evidence that the allometric effect on cranial shape is not sexually dimorphic. MNHN 6994 has a much larger cranial centroid size and more extreme shape than the other sampled specimens, though it falls along the same linear relationship (Figure S2). Based on Procrustes distance from the mean, this specimen is an outlier, and it was removed from subsequent analyses.

The corresponding scatterplot of the regression of tail-shield $\log_{10}$-transformed centroid size against shape also presents a linear relationship (Figure S3), although weaker at larger centroid sizes. At greater centroid sizes, tail-shields are more acutely conical. There is no indication of sexual dimorphism in the allometric effect on tail-shield shape, as shown by the lack of separate clustering of males and females. BMNH 1964.1701 is an outlier in the regression plot, which was expected given its much less well ossified and notably irregularly shaped tail-shield (Figure S1). This specimen was removed from subsequent analyses.

3.3 | Cranial and bony tail-shield shape variation

Twenty-nine PC scores were required to explain 99% of cranial shape variation (Table S4) and differences in adjusted cranial shape at the minimum and maximum distributions along each axis are subtle (Figure 4a, Figures S4–S7). PC1 accounts for only 13.03% of the overall variation. Crania with highest positive values on this axis have a less spherical occipital condyle, a wider posterior process of the pterygoid, a taller septomaxilla and a more pronounced sloping of the premaxilla anteroventrally from the nasal process (Figure 4a and Figure S4). PC2, accounting for

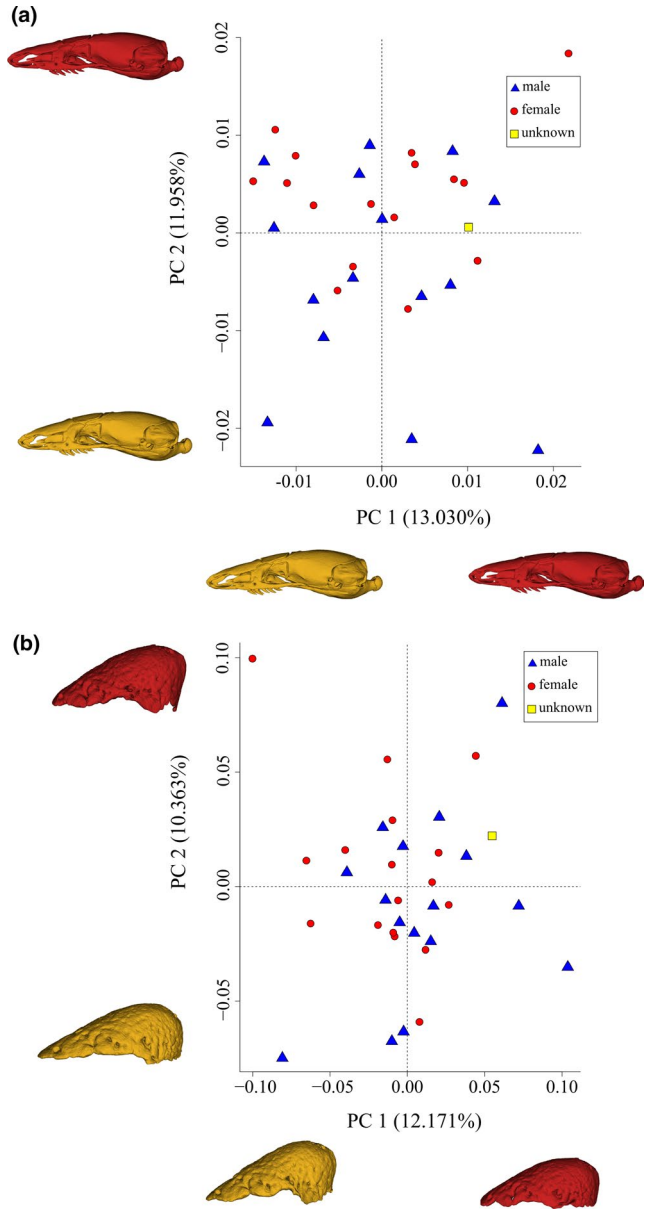

FIGURE 4 Morphospaces of (a) adjusted cranial shape and (b) adjusted bony tail-shield shape in *Rhinophis philippinus* constructed from PC1 and PC2 axes. Crania and tail-shields with the minimum (yellow) and maximum (red) values for of each PC axis are displayed in lateral view. For tail-shield views, posterior is to the top

11.96% of variation, is associated with differences in the dorsal longitudinal arch of the braincase, whereby crania at higher positive values along this axis have a lower dorsal arching in lateral view (Figure 4a and Figure S5); they also have a longer palatine and a relatively wider premaxilla. Specimens located at the negative extreme of PC2 are represented by three males (Figure 4a) with a clearly higher dorsal arch to the braincase. PC3, accounting for 9.22% of variation, is associated with differences in the position of the pterygoid, with crania at the far positive end of PC3 having relatively lower posterior ends of the pterygoids seen in lateral view (Figures S6 and S7).

No clustering of the sexes is displayed in the cranial morphospace of PC1 versus PC2 (Figure 4a). Thus, there is no evidence for sexual dimorphism in adjusted cranial shape in *R. philippinus*. Consequently, no inferences can be made as to the sex of the single specimen (BMNH 1964.1705) for which sex was not known. This was the only specimen with a somewhat intermediate relative tail length, and unambiguously male or female urogenital features could not be located.

Thirty PC scores were required to explain 99% of the variation in bony tail-shield morphology (Table S5). Identifying the aspects of shape variation explained by each PC axis is simpler than for cranial variation. PC1, accounting for 12.17% of variation, describes primarily the shape of the posterior projection of the shield in dorsal view, with shields at the far positive end of this axis being more broadly rounded with a blunter posterior edge, along with a less complex free edge and less extended transverse processes on the vertebrae (Figure 4B and Figure S8). PC2, associated with 10.36% of variation, relates to differences in the projection of the bony-shield's dome, with shields at the far positive end of this axis being more acutely conical (Figure 4b and Figure S9). PC3, accounting for 8.35% of variation, describes differences in the width and length of the shield, with those at the far positive end of this axis having a wider and shorter shield (Figures S10 and S11).

All specimens are distributed evenly throughout a tail-shield morphospace plot of PC1 versus PC2 (Figure 4b). There is no clustering of the sexes, such that there is no evidence of sexual dimorphism in the adjusted tail-shield shape in *R. philippinus*.

3.4 | Covariation between cranial and bony-shield shape

Covariation between cranial and bony tail-shield shape was significant when using adjusted shape data (*r-PLS* = 0.85, p = 0.03) and shape data (*r-PLS* = 0.85, p = 0.001). Most of the covariation in the shape dataset was explained by the first axis (62.84%), with the majority of the covariation in the adjusted shape dataset spread over the first three axes (22.47%, 16.21%, and 12.05%).

The scatterplots of the results of each 2B-PLS analysis show a positive linear relationship between cranial adjusted shape and bony-shield adjusted shape. For the adjusted shape data analysis, crania at the positive end of the PLS axis are slightly more pointed with a less dorsally arched skull roof in lateral view. These cranial shapes are associated with more acutely conical bony shields (Figure 5a). No sexual dimorphism is apparent in this covariation scatterplot.

The shape data analysis finds a similar pattern of covariation between the cranial and bony-shield shape, though with significantly more pronounced differences in shape at the ends of each axis (Figure 5b). Here, crania with high positive PLS scores have less dorsally arched roofs in lateral view, relatively larger maxillae, an elongated snout, a posteriorly flared exoccipital arch, and a larger and more bulbous occipital condyle in lateral view. The minimum and maximum PLS scores for bony shields are associated with flatter and with more acutely conical shapes, respectively.

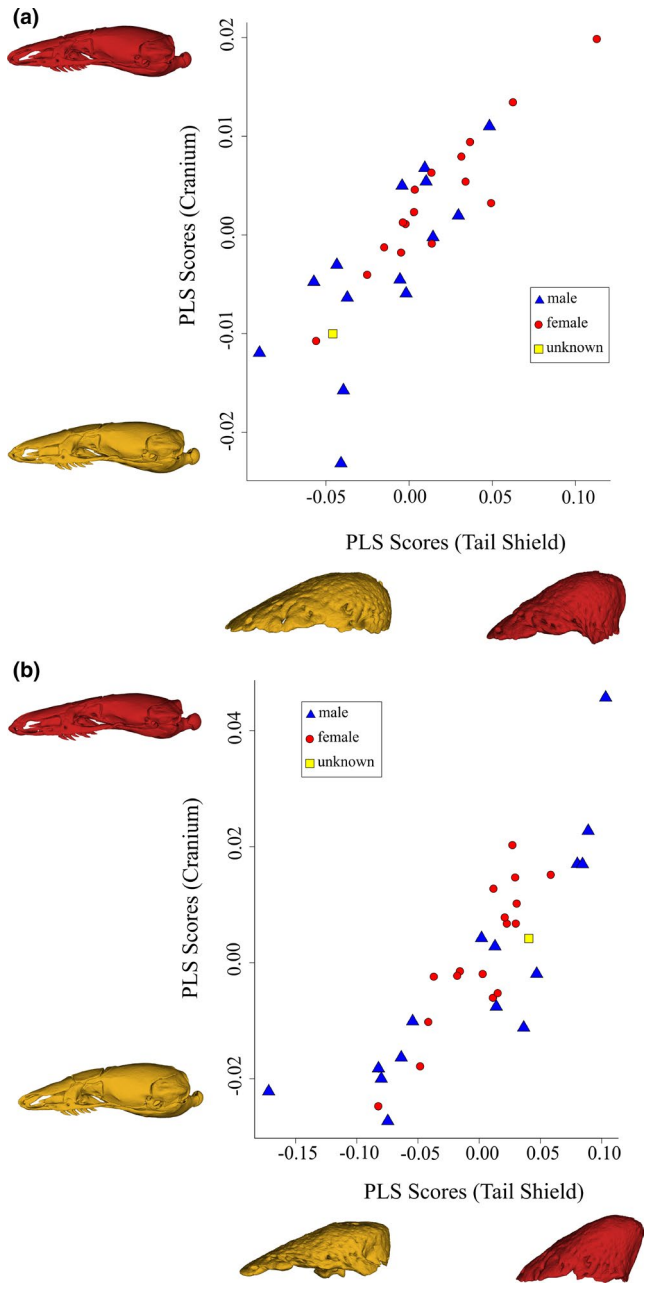

FIGURE 5 Results of two-block partial least squares analyses of cranial and bony tail-shield shape in *Rhinophis philippinus*, using (a) adjusted shape data and (b) shape data. Cranial and tail-shield conformations, in lateral view, are for specimens at the extreme negative (yellow) and positive (red) ends of each block of PLS score axes. For tail-shield views, posterior is to the top

3.5 | Sexual dimorphism tests for crania and bony tail-shields

Male and female specimens have very similar levels of adjusted shape variation (crania Pv = 0.00072 and 0.00063, respectively; tail-shield Pv = 0.01327 and 0.01342, respectively), with no significant difference in disparity (crania p = 0.182, tail-shield p = 0.925). Therefore, there is no evidence of sexual dimorphism displayed in the shape disparity of these structures in *R. philippinus*.

MANOVA found no adjusted shape differences depending on sex for both crania and bony tail-shields (F = 1.25, p = 0.171 and F = 1.379, p = 0.078, respectively). This is consistent with the lack of separation of male and female specimens in the morphospaces (Figure 4). The results of the analyses of variance performed on both the $\log_{10}$-transformed centroid size of crania and bony shields are also non-significant (ANOVA: F = 0.003, p = 0.962 and F = 0.265, p = 0.618, respectively).

3.6 | Correlation between centroid size and external morphology

SVL and cranial centroid size are moderately positively correlated (rho_S = 0.490, p = 0.004), while SVL and bony-shield centroid size are less positively correlated (rho_S = 0.341, p = 0.045). There is a low positive correlation also between tail length and cranial centroid size (rho_S = 0.192, p = 0.284), and between tail length and bony-shield centroid size (rho_S = 0.238, p = 0.168). Head length and cranial centroid size are moderately positively correlated (rho_S = 0.524, p = 0.002).

4 | DISCUSSION

Fossorial vertebrates that have reduced or no limbs have long been recognized to have accumulated cranial specializations associated with head-first burrowing. These have been studied quantitatively in taxa as diverse as caecilians (Gymnophiona: (Bardua et al., 2019; Marshall et al., 2019; Sherratt et al., 2014), worm lizards (Amphisbaenidae: (Hipsley et al., 2016), and eels (Moringuidae: (De Schepper et al., 2005). However, thus far, cranial morphology has not been investigated thoroughly or from a quantitative perspective in Uropeltidae, a major group of fossorial snakes. The little previous research into variation in uropeltid cranial morphology has been restricted mostly to qualitative characters and interspecific variation (Cundall & Irish, 2008; Olori, 2010; Olori & Bell, 2012; Rieppel, 1977, 1978, 1979; Rieppel & Zaher, 2002). Investigation into tail-shield osteology of Uropeltidae has been non-existent beyond Baumeister's early study (1908), representing a missed opportunity to understand the origins and function of the puzzling tail specializations of this family of snakes. For the first time, our study applied a geometric morphometric approach to analyze intraspecific variation in uropeltid cranial and bony tail-shield shape. As far as we are aware, this is also the first quantitative test of sexual dimorphism in head and tail-shield size and shape in uropeltids. The results provide novel insights into the major morphological variations in *Rhinophis* that have implications for understanding sexual dimorphism and tail-shield function.

4.1 | Sexual dimorphism

Our study found no evidence of sexual dimorphism in the size or shape of the head, cranium, external tail shield, bony tail-shield, or

SVL in the available sample of *R. philippinus*. This finding might be considered surprising given that sexual dimorphism is prevalent in snakes, in general, particularly with regards to size (Fitch, 1981; King, 1989; Shine, 1994). Similar head and cranial shape and size in male and female *R. philippinus* may indicate a trade-off between ecological and sexual selection, should the latter exist in this species. Some studies have shown that the selective pressures generated by head-first burrowing and a fossorial lifestyle might have a larger impact on head and cranial morphology than does any sexual selection. Studies establishing the presence or absence of sexual dimorphism in other species of Uropeltidae could provide further tests of this possible trade-off. Among other head-first burrowing, limbless vertebrates, sexual dimorphism has been found in head or cranial shape in only some amphisbaenians (Hipsley et al., 2016) and in some caecilian amphibians. The causes and consequences are poorly understood in these typically little-studied animals. However, male *Schistometopum thomense* tend to have larger heads that are costly in terms of burrowing speed (Teodecki et al., 1998), and head dimorphism in *Boulengerula boulengeri* is associated with dimorphism in diet (Jones et al., 2006). Lack of sexual dimorphism in *R. philippinus* cranial shape suggests a homogeneity in burrowing ability and diet between males and females, something that is open to testing in the field and/or laboratory. It is important to note that sexual dimorphism is complex and can be generated from several different drivers that are not mutually exclusive, including sexual selection (Darwin, 1871; Olsson et al., 2002), male-male combat (Shine, 1978), or ecological niche divergence between the sexes (Slatkin, 1984; Vincent et al., 2004). Interpretations of the potential drivers of sexual dimorphism solely based on shape and size variation thus are tentative as acquisition of in vivo data are needed to test these hypotheses.

The lack of sexual dimorphism in tail-shield shape suggests that this structure in uropeltids, or at least *R. philippinus*, performs a common function in both sexes. Therefore, from this, it can be postulated that tail-shields serve no role in sexual selection in *R. philippinus*, and instead are more likely to function in locomotion and/or predator avoidance. Uropeltid snakes are known to be preyed on by boars and birds (Rajendran, 1985), and it has been argued that the cephalic mimicry of the tail-shield directs potential attacks from these predators away from the head and toward this more resilient structure (Cyriac & Kodandaramaiah, 2019; Gans, 1986a; Melvinselvan & Nibedita, 2016).

Although there is no dimorphism in external shield shape, there is pronounced sexual dimorphism in tail length, with males having longer tails than females. This can be explained by the uneverted hemipenes of male squamates being stored in the base of the tail (Shine et al., 1999). Male-male "tail wrestling" combat (Shine et al., 1999) seems unlikely in snakes with very short tails, as in *Rhinophis*, and has not been reported in uropeltids, but longer tails perhaps also help functionally in attaining cloacal apposition during initial stages of copulation. The latter could be tested with data on male reproductive success and/or body condition in relation to tail length (Sivan et al., 2020). As pointed out by Jins et al. (2018), the higher number of ventral scales in females can be explained by selective pressure for increased space for fetal gestation, all uropeltids being viviparous as far as is known (Rajendran, 1985).

4.2 | Shape variation in crania and bony tail-shields

Variation in both cranial and bony-shield morphology in *R. philippinus* is significantly correlated with size, with allometry accounting for 23.8% and 15.1% of the shape variation, respectively. This allometric effect in the skull was characterized by larger crania being longer and narrower, particularly toward the posterior of the skull. Pointed heads are common in limbless fossorial vertebrates, often being more effective for head-first burrowing (Gans, 1994; Haas et al., 2006; Lopez et al., 1997; Rodrigues et al., 2016; Roscito & Rodrigues, 2010; Sherratt et al., 2014; Shimer, 1903). Pronounced allometry, with less acutely pointed crania and wider braincases in smaller specimens, is possibly explained by constraints in minimum functional size of sensory structures held in the back of the skull, such as the inner ear (Olori, 2010). Alternatively, larger crania may be relatively narrower to account for the greater effort required to move a larger body through the substrate.

MNHN 6994 is by far the largest specimen in the sample (total length 259 mm versus 211 mm for one other specimen and all others <200 mm), and allometric analyses identified this individual as also having a significantly larger cranial centroid size (66.3 mm versus mean of 47.9 mm in other specimens). There is no indication that the skull of MNHN 6994 (the holotype of the species) represents a species different from that of the other specimens because it is qualitatively similar in its osteology and external morphology, and does not depart from the same allometric regression line (Figure S2). However, the collection localities of all but two specimens in our sample are unknown, and we have little to no understanding of uropeltid demographics, ontogeny, and geographical morphological variation. Thus, it remains possible that our study lacks sufficient sampling of total lengths and or populations to detect other patterns of variation among specimens currently referable to *R. philippinus*.

Variation in cranial shape of *R. philippinus* is spread broadly across many axes, in contrast with findings from a wider squamate study in which almost two-thirds of cranial shape variation is explained by the first three PC axes (Watanabe et al., 2019). This is likely explained by the intraspecific sampling of this study and by the generally conserved cranial osteology within *R. philippinus*, including a lack of sexual dimorphism. The *R. philippinus* cranial variation across the first few axes encompass differences in the occipital condyle shape, the size and position of the pterygoid (though we note this could be an artifact of how the specimens are preserved) and the longitudinal arching of the braincase roof. Little variation is present in the shape of the snout, which may be highly conserved due to its function in head-first burrowing in these snakes. Cranial shape variation can be dependent upon

the nature of the substrate in which a limbless fossorial organism burrows (Greenville & Dickman, 2009; Jackson et al., 2008). Most uropeltids, including *R. philippinus* (DJG, pers. obs.), tend to be found in moist, clay- and/or humus-rich soils (Rajendran, 1985), but no studies have been conducted to determine microhabitat tolerances or preferences in this family of snakes.

Larger (and presumably older) bony tail-shields are more acutely conical, but without more research, it is unclear how patterns of ossification may influence this shape and any functional consequences possibly associated with this. Variation in bony-shield shape was, as with the cranium, similarly spread over many axes, which is also likely to be explained by the intraspecific dataset and conserved shape of this structure, including lack of sexual dimorphism. Pyron et al. (2016) reported ontogenetic variation in the external keratinous shield of *Rhinophis melanogaster*, with smaller specimens having a relatively much smaller shield, but no quantitative data or analyses were presented. Broader taxon sampling will allow a better understanding of the patterns and causes of shield size and shape variation within and among species.

Although the overall variation in both the crania and the tail-shields is slight and subtle in *R. philippinus*, there is a significant covariation between the two structures, with a longer, narrower cranium being associated with a more conical tail-shield. However, given that this relationship is more exaggerated in the shape data that were not corrected for allometry, a large proportion of this covariation is likely due to covariation in size.

The use of geometric morphometrics provides a highly detailed approach to quantifying shape variation, especially with the use of sliding semilandmarks (Goswami et al., 2019). Although the number of landmarks and semilandmarks used on the tail-shield was sufficient to investigate the whole shape, it would have been useful to repeat the cranial analyses with the addition of surface semilandmarks to investigate whether that increased coverage better captured morphological variation.

It is interesting to note that centroid size, issued from the cranial and bony-shield shape analyses, is not a good proxy of the overall size of the individual *R. philippinus*, either for SVL or tail length. Furthermore, due to the decoupling of the head from the body in elongate animals (Sherratt et al., 2019), it might be expected that cranial centroid size would be a good proxy for head length; however, we found little correlation between these measurements. Thus, future analyses could substitute centroid size with tail length as a covariate in sex differentiation analyses, and SVL or total length for the impact of size on shape.

Our study provides new insights into intraspecific variation of this very poorly known genus and family of snakes and has prompted several questions worthy of future research. The main limitations of this study are the lack of ecological and behavioral data for *R. philippinus*, the lack of knowledge about geographic provenance of all but two of the sampled specimens, the lack of male specimens of total length >200 mm, and the paucity of information regarding the natural history of this species. Future studies of *R. philippinus* variation might aim to remedy these, as well as expand analyses of variation to other aspects of external morphology and osteology, including lower jaws. In addition, similar studies are required for other uropeltid taxa to determine whether the patterns found here extend to the whole family. *Rhinophis* species have some of the most extreme head and tail-shield morphologies within Uropeltidae and morphological variation within *R. philippinus* might not be typical. Some species of other uropeltid genera are more strikingly colored than *R. philippinus* and might be less dedicated burrowers, spending more time on the surface (Cyriac & Kodandaramaiah, 2020). Thus, similar studies of morphological variation for those species would provide a test of the hypothesis that morphological variation in the head and cranium of *R. philippinus* can be explained by strong stabilizing selection to maintain an optimum morphology for head-first burrowing. Finally, further studies of uropeltids in the field, in captivity and the laboratory are required to help identify causes of the patterns of morphological variation that are discovered.

ACKNOWLEDGEMENTS

LCH thanks Carla Bardua, Gizeh Rangel de Lázaro, Ellen J. Coombs, and Andrew Knapp for advice and guidance with computer software and methods. Matthew J. Mitchell and Sarah Cockerill are also thanked for their helpful support during both the analytical and writing stages. Brett Clark, Vincent Fernandez and Farah Ahmed (NHM, London), and Maïté Adam and Antoine Balzeau (MNHN, Paris) are thanked for help with generating micro-CT data. DJG and FLS thank Nicolas Vidal and colleagues for access to MNHN specimens. FLS's contribution was funded by a London NERC DTP PhD studentship (ref: NE/ L002485/1; co-supervised by Julia Day), a UCL Bogue Fellowship, and a Systematics Research Fund grant from the UK's Systematics Association and the Linnean Society of London. FLS's and DJG's visit to MNHN was funded by the EU SYNTHESYS scheme. This work was supported in part by ERC grant STG-2014-637171 to AG. Jennifer Olori and Vivek Philip Cyriac are thanked for constructively critical, expert reviews of the submitted manuscript.

ORCID

Lucy C. Huntley https://orcid.org/0000-0002-9135-1054
David J. Gower https://orcid.org/0000-0002-1725-8863
Filipa L. Sampaio https://orcid.org/0000-0002-7451-8318
Anjali Goswami https://orcid.org/0000-0001-9465-810X
Anne-Claire Fabre https://orcid.org/0000-0001-7310-1775

REFERENCES

Adams, D., Collyer, M., & Kaliontzopoulou, A. (2020). *Geomorph: Software for geometric morphometric analyses. R package version 3.2.1*. https://cran.r-project.org/package=geomorph

Adler, D., Murdoch, D., Nenadic, O., Urbanek, S., Chen, M., Gebhardt, A., Bolker, B., Csardi, G., Strzelecki, A., Senger, A., & Eddelbuettel, D. (2020). *Package 'rgl' (Version 0.100.50)*. https://r-forge.r-project.org/projects/rgl/

Alexander, A. A., & Gans, C. (1966). The pattern of dermal-vertebral correlation in snakes and amphisbaenians. *Zoologische Mededelingen*, *41*(11), 171–190.

Bardua, C., Wilkinson, M., Gower, D. J., Sherratt, E., & Goswami, A. (2019). Morphological evolution and modularity of the caecilian skull. *BMC Evolutionary Biology*, *19*(1), 30. https://doi.org/10.1186/s12862-018-1342-7

Baumeister, L. (1908). Beitrage zur Anatomie und Physiologie der Rhinophiden. *Zoologische Jahrbuch, Abteilung Anatomie*, *26*, 423–526.

Bookstein, F. L. (1989). Principal warps: Thin-plate splines and the decomposition of deformations. *IEEE Transactions on Pattern Analysis and Machine Intelligence*, *11*(6), 567–585. https://doi.org/10.1109/34.24792

Bookstein, F. L. (1992). Landmarks. In *Morphometric tools for landmark data: Geometry and biology* (pp. 55–87). Cambridge: Cambridge University Press.

Boulenger, G. A. (1893). *Catalogue of the snakes in the British Museum (Natural History) (Vol. v. 1)*. London: Taylor & Francis.

Burbrink, F. T., Grazziotin, F. G., Pyron, R. A., Cundall, D., Donnellan, S., Irish, F., Keogh, J. S., Kraus, F., Murphy, R. W., Noonan, B., Raxworthy, C. J., Ruane, S., Lemmon, A. R., Lemmon, E. M., & Zaher, H. (2020). Interrogating genomic-scale data for Squamata (lizards, snakes, and amphisbaenians) shows no support for key traditional morphological relationships. *Systematic Biology*, *69*(3), 502–520. https://doi.org/10.1093/sysbio/syz062

Clark, D. R. (1966). Notes on sexual dimorphism in tail-length in American snakes. *Transactions of the Kansas Academy of Science (1903-)*, *69*(3/4), 226–232. https://doi.org/10.2307/3627419

Comeaux, R. S., Olori, J. C., & Bell, C. J. (2010). Cranial osteology and preliminary phylogenetic assessment of *Plectrurus aureus* Beddome, 1880 (Squamata: Serpentes: Uropeltidae). *Zoological Journal of the Linnean Society*, *160*(1), 118–138. https://doi.org/10.1111/j.1096-3642.2009.00595.x

Constable, J. D. (1949). Reptiles from the Indian Peninsula in the Museum of Comparative Zoology. In Z. Harvard University. Museum of Comparative (Ed.), *Bulletin of the museum of comparative Zoology at Harvard College* (Vol. *103*, pp. 59–160). The Museum.

Cundall, D., & Irish, F. (2008). The snake skull. In C. Gans, A. Gaunt, & K. Adler (Eds.), *Biology of the reptilia* (Vol. *20*, pp. 349–692). Morphology H.

Cuvier, G. B., & Latreille, P. A. (1829). *Le règne animal distribué d'après son organisation, pour servir de base à l'histoire naturelle des animaux et d'introduction à l'anatomie comparée (Nouvelle édition rev. et aug. ed.)*. Chez Déterville.

Cyriac, V. P., & Kodandaramaiah, U. (2019). Conspicuous colours reduce predation rates in fossorial uropeltid snakes. *PeerJ*, *7*, e7508. https://doi.org/10.7717/peerj.7508

Cyriac, V. P., & Kodandaramaiah, U. (2020). Warning signals promote morphological diversification in fossorial uropeltid snakes (Squamata: Uropeltidae). *Zoological Journal of the Linnean Society*, *191*(2), 468–481. https://doi.org/10.1093/zoolinnean/zlaa062

Cyriac, V. P., Narayanan, S., Sampaio, F. L., Umesh, P., & Gower, D. J. (2020). A new species of *Rhinophis* Hemprich, 1820 (Serperates: Uropeltidae) from the Wayanad region of peninsular India. *Zootaxa*, *4778*(2), 329–342. https://doi.org/10.11646/zootaxa.4778.2.5

Da Silva, F. O., Fabre, A.-C., Savriama, Y., Ollonen, J., Mahlow, K., Herrel, A., Müller, J., & Di-Poï, N. (2018). The ecological origins of snakes as revealed by skull evolution. *Nature Communications*, *9*(1), 376. https://doi.org/10.1038/s41467-017-02788-3

Darwin, C. (1871). *The descent of man, and selection in relation to sex*. John Murray.

De Schepper, N., Adriaens, D., & De Kegel, B. (2005). *Moringua edwardsi* (Moringuidae: Anguilliformes): Cranial specialization for head-first burrowing? *Journal of Morphology*, *266*(3), 356–368. https://doi.org/10.1002/jmor.10383

Delêtre, M., & Measey, J. (2004). Sexual selection vs. ecological causation in a sexually dimorphic caecilian, *Schistometopum thomense* (Amphibia: Gymnophiona: Caeciliidae). *Ethology Ecology and Evolution*, *16*, 243–253. https://doi.org/10.1080/08927014.2004.9522635

Fabre, A.-C., Andrade, D. V., Huyghe, K., Cornette, R., & Herrel, A. (2014). Interrelationships between bones, muscles, and performance: Biting in the lizard *Tupinambis merianae*. *Evolutionary Biology*, *41*(4), 518–527. https://doi.org/10.1007/s11692-014-9286-3

Fabre, A.-C., Cornette, R., Huyghe, K., Andrade, D. V., & Herrel, A. (2014). Linear versus geometric morphometric approaches for the analysis of head shape dimorphism in lizards. *Journal of Morphology*, *275*(9), 1016–1026. https://doi.org/10.1002/jmor.20278

Fitch, H. S. (1981). *Sexual size differences in reptiles* (Vol. *70*). Miscellaneous publication - University of Kansas, Museum of Natural History.

Gans, C. (1976). Aspects of the biology of uropeltid snakes. In A. Bellairs, & C. B. Cox (Eds.), *Morphology and biology of reptiles* (pp. 191–204). Linnean Society Symposium Academic Press.

Gans, C. (1986a). Automimicry and Batesian mimicry in uropeltid snakes: Pigment pattern, proportions, and behavior. *Journal of the Bombay Natural History Society*, *83*, 152–158.

Gans, C. (1986b). Functional morphology of predator-prey relationships. In M. E. Feder, & G. V. Lauder (Eds.), *Predator-prey relationships. Perspectives and approaches from the study of lower vertebrates* (pp. 6–23). The University of Chicago Press.

Gans, C. (1994). Approaches to the evolution of limbless locomotion. *Cuadernos de Herpetología*, *8*(1), 12–17.

Gans, C., & Baic, D. (1977). Regional specialization of reptilian scale surfaces: Relation of texture and biologic role. *Science*, *195*(4284), 1348. https://doi.org/10.1126/science.195.4284.1348

Goswami, A., Watanabe, A., Felice, R. N., Bardua, C., Fabre, A.-C., & Polly, P. D. (2019). High-density morphometric analysis of shape and integration: The good, the bad, and the not-really-a-problem. *Integrative and Comparative Biology*, *59*(3), 669–683. https://doi.org/10.1093/icb/icz120

Gower, D. J. (2020). A new species of *Rhinophis* Hemprich, 1820 (Serpentes: Uropeltidae) from southwestern Sri Lanka. *Zootaxa*, *4810*, 495–510. https://doi.org/10.11646/zootaxa.4810.3.6

Gower, D. J., & Ablett, J. D. (2006). Counting ventral scales in Asian anilioid snakes. *Herpetological Journal*, *16*, 259–263.

Gower, D. J., Captain, A., & Thakur, S. S. (2008). On the taxonomic status of *Uropeltis bicatenata* (Günther) (Reptilia: Serpentes: Uropeltidae). *Hamadryad*, *33*, 64–82.

Gower, D. J., Giri, V., Captain, A., & Wilkinson, M. (2016). A reassessment of *Melanophidium* Günther, 1864 (Reptilia: Serpentes: Uropeltidae) from the Western Ghats of peninsular India, with the description of a new species. *Zootaxa*, *4085*, 481–503. https://doi.org/10.11646/zootaxa.4085.4.2

Greenville, A. C., & Dickman, C. R. (2009). Factors affecting habitat selection in a specialist fossorial skink. *Biological Journal of the Linnean Society*, *97*(3), 531–544. https://doi.org/10.1111/j.1095-8312.2009.01241.x

Guibé, J. (1948). Étude du dimorphisme sexuel chez trois espèces du genre *Silybura* (Ophidien). *Bulletin de la Societé Zoologique de France*, *73*, 91–94.

Haas, A., Hertwig, S., & Das, I. (2006). Extreme tadpoles: The morphology of the fossorial megophryid larva, *Leptobrachella mjobergi*. *Zoology*, *109*(1), 26–42. https://doi.org/10.1016/j.zool.2005.09.008

Heideman, N. J. L, Daniels, S. R., Mashinini, P. L., Mokone, M. E., Thibedi, M. L., Hendricke, M. G. J., Wilson, B. A., & Douglas, R. M. (2008). Sexual dimorphism in the African legless skink subfamily Acontiinae (Reptilia: Scincidae). *African Zoology*, *43*(2), 192–201. https://doi.org/10.1080/15627020.2008.11657236

Hipsley, C. A., Rentinck, M. N., Rodel, M. O., & Muller, J. (2016). Ontogenetic allometry constrains cranial shape of the head-first burrowing worm lizard *Cynisca leucura* (Squamata: Amphisbaenidae). *Journal of Morphology*, *277*(9), 1159–1167. https://doi.org/10.1002/jmor.20564

Jackson, C. R., Lubbe, N. R., Robertson, M. P., Setsaas, T. H., Van Der Waals, J., & Bennett, N. C. (2008). Soil properties and the distribution of the endangered Juliana's golden mole. *Journal of Zoology*, *274*(1), 13–17. https://doi.org/10.1111/j.1469-7998.2007.00351.x.

Jins, V. J., Sampaio, F. L., & Gower, D. J. (2018). A new species of *Uropeltis* Cuvier, 1829 (Serpentes: Uropeltidae) from the Anaikatty Hills of the Western Ghats of India. *Zootaxa*, *4415*(3), 401–422. https://doi.org/10.11646/zootaxa.4415.3.1

Jones, D. T., Loader, S. P., & Gower, D. J. (2006). Trophic ecology of East African caecilians (Amphibia: Gymnophiona), and their impact on forest soil invertebrates. *Journal of Zoology*, *269*(1), 117–126. https://doi.org/10.1111/j.1469-7998.2006.00045.x

Kaliontzopoulou, A., Carretero, M. A., & Llorente, G. A. (2007). Multivariate and geometric morphometrics in the analysis of sexual dimorphism variation in *Podarcis* lizards. *Journal of Morphology*, *268*(2), 152–165. https://doi.org/10.1002/jmor.10494

King, R. B. (1989). Sexual dimorphism in snake tail length: Sexual selection, natural selection, or morphological constraint? *Biological Journal of the Linnean Society*, *38*(2), 133–154. https://doi.org/10.1111/j.1095-8312.1989.tb01570.x

Klingenberg, C. P. (2016). Size, shape, and form: Concepts of allometry in geometric morphometrics. *Development Genes and Evolution*, *226*(3), 113–137. https://doi.org/10.1007/s00427-016-0539-2

Lopez, P., Martin, J., & Barbosa, A. (1997). State and morphological dependent escape decisions in a fossorial lizard. *Journal of Morphology*, *232*(3), 289. https://doi.org/10.1002/(SICI)1097-4687(199706)232:3<281:AID-JMOR8>3.0.CO;2-A

Lucas, T., & Goswami, A. (2017). *paleomorph: Geometric morphometric tools for Paleobiology (Version 0.1.4)*. https://github.com/timcdlucas/paleomorph/

Marshall, A. F., Bardua, C., Gower, D. J., Wilkinson, M., Sherratt, E., & Goswami, A. (2019). High-density three-dimensional morphometric analyses support conserved static (intraspecific) modularity in caecilian (Amphibia: Gymnophiona) crania. *Biological Journal of the Linnean Society*, *126*(4), 721–742. https://doi.org/10.1093/biolinnean/blz001

Melvinselvan, G., & Nibedita, D. (2016). Defensive caudal display in *Uropeltis pulneyensis* Beddome 1863 (Serpentes: Uropeltidae) from Palani Hills, Western Ghats. *India. Russian Journal of Herpetology*, *23*(1), 77–80. https://doi.org/10.30906/1026-2296-2016-23-1-77-80

Miralles, A., Marin, J., Markus, D., Herrel, A., Hedges, S. B., & Vidal, N. (2018). Molecular evidence for the paraphyly of Scolecophidia and its evolutionary implications. *Journal of Evolutionary Biology*, *31*(12), 1782–1793. https://doi.org/10.1111/jeb.13373

Olori, J. C. (2010). Digital endocasts of the cranial cavity and osseous labyrinth of the burrowing snake *Uropeltis woodmasoni* (Alethinophidia: Uropeltidae). *Copeia*, *2010*(1), 14–26. https://doi.org/10.1643/CH-09-082

Olori, J. C., & Bell, C. J. (2012). Comparative skull morphology of uropeltid snakes (Alethinophidia: Uropeltidae) with special reference to disarticulated elements and variation. *PLoS One*, *7*(3), e32450. https://doi.org/10.1371/journal.pone.0032450

Olsson, M., Shine, R., Wapstra, E., Ujvari, B., & Madsen, T. (2002). Sexual dimorphism in the lizard body shape: The roles of sexual selection and fecundity selection. *Evolution*, *56*(7), 1538–1542. https://doi.org/10.1111/j.0014-3820.2002.tb01464.x

Parr, W. C. H., Wroe, S., Chamoli, U., Richards, H. S., McCurry, M. R., Clausen, P. D., & McHenry, C. (2012). Toward integration of geometric morphometrics and computational biomechanics: New methods for 3D virtual reconstruction and quantitative analysis of Finite Element Models. *Journal of Theoretical Biology*, *301*, 1–14. https://doi.org/10.1016/j.jtbi.2012.01.030

Pyron, R. A., Ganesh, S. R., Sayyed, A., Sharma, V., Wallach, V., & Somaweera, R. (2016). A catalogue and systematic overview of the shield-tailed snakes (Serpentes: Uropeltidae). *Zoosystema*, *38*(4), 453–506. https://doi.org/10.5252/z2016n4a2

R Core Team (2019). *A language and environment for statistical computing (Version 3.6.1)*. R Foundation for Statistical Computing. https://www.R-project.org/

Rajendran, M. (1985). *Studies in Uropeltid snakes*. Madurai Kamaraj University.

Rieppel, O. (1977). Studies on the skull of the Henophidia (Reptilia: Serpentes). *Journal of Zoology*, *181*, 145–173. https://doi.org/10.1111/j.1469-7998.1977.tb03235.x

Rieppel, O. (1978). The evolution of the naso-frontal joint in snakes and its bearing on snake origins. *Journal of Zoological Systematics and Evolutionary Research*, *16*(1), 14–27. https://doi.org/10.1111/j.1439-0469.1978.tb00917.x

Rieppel, O. (1979). The evolution of the basicranium in the Henophidia (Reptilia: Serpentes). *Zoological Journal of the Linnean Society*, *66*(4), 411–431. https://doi.org/10.1111/j.1096-3642.1979.tb01915.x

Rieppel, O., & Zaher, H. (2002). The skull of the Uropeltinae (Reptilia, Serpentes), with special reference to the otico-occipital region. *Bulletin of the Natural History Museum. Zoology Series*, *68*(2), 123–130. https://doi.org/10.1017/S0968047002000146

Rivas, J., & Burghardt, G. (2001). Understanding sexual size dimorphism in snakes: Wearing the snake's shoes. *Animal Behaviour*, *62*, F1–F6. https://doi.org/10.1006/anbe.2001.1755

Rodrigues, H. G., Šumbera, R., & Hautier, L. (2016). Life in burrows channelled the morphological evolution of the skull in rodents: The case of African mole-rats (Bathyergidae, Rodentia). *Journal of Mammalian Evolution*, *23*(2), 175–189. https://doi.org/10.1007/s10914-015-9305-x

Rohlf, F. J., & Corti, M. (2000). Use of two-block partial least-squares to study covariation in shape. *Systematic Biology*, *49*(4), 740–753. https://doi.org/10.1080/106351500750049806

Rohlf, F. J., & Slice, D. (1990). Extensions of the Procrustes method for the optimal superimposition of landmarks. *Systematic Zoology*, *39*(1), 40–59. https://doi.org/10.2307/2992207

Roscito, J. G., & Rodrigues, M. T. (2010). Comparative cranial osteology of fossorial lizards from the tribe Gymnophthalmini (Squamata, Gymnophthalmidae). *Journal of Morphology*, *271*(11), 1352–1365. https://doi.org/10.1002/jmor.10878

Sampaio, F. L., Narayanan, S., Cyriac, V. P., Govindappa, V., & Gower, D. (2020). A new Indian species of *Rhinophis* Hemprich, 1820 closely related to *R. sanguineus* Beddome, 1863 (Serpentes: Uropeltidae). *Zootaxa*, *488*, 001–024. https://doi.org/10.11646/zootaxa.4881.1.1

Schlager, S. (2017). *Morpho and Rvcg – Shape analysis in R*. Academic Press.

Sherratt, E., Coutts, F. J., Rasmussen, A. R., & Sanders, K. L. (2019). Vertebral evolution and ontogenetic allometry: The developmental basis of extreme body shape divergence in microcephalic sea snakes. *Evolution and Development*, *21*(3), 135–144. https://doi.org/10.1111/ede.12284

Sherratt, E., Gower, D. J., Klingenberg, C. P., & Wilkinson, M. (2014). Evolution of cranial shape in caecilians (Amphibia: Gymnophiona). *Evolutionary Biology*, *41*(4), 528–545. https://doi.org/10.1007/s11692-014-9287-2

Shimer, H. W. (1903). Adaptations to aquatic, arboreal, fossorial and cursorial habits in mammals. III. Fossorial adaptations. *The American Naturalist*, *37*(444), 819–825. https://doi.org/10.1086/278368

Shine, R. (1978). Sexual size dimorphism and male combat in snakes. *Oecologia*, *33*(3), 269–277. https://doi.org/10.1007/bf00348113

Shine, R. (1994). Sexual size dimorphism in snakes revisited. *Copeia*, *1994*(2), 326–346. https://doi.org/10.2307/1446982

Shine, R., Olsson, M. M., Moore, I. T., LeMaster, M. P., & Mason, R. T. (1999). Why do male snakes have longer tails than females? *Proceedings of the Royal Society B: Biological Sciences*, *266*(1434), 2147. https://doi.org/10.1098/rspb.1999.0901

Sivan, J., Hadad, S., Tesler, I., Rosenstrauch, A., Allan Degen, A., & Kam, M. (2020). Relative tail length correlates with body condition in male but not in female crowned leafnose snakes (*Lytorhynchus diademα*). *Scientific Reports*, *10*(1), 4130. https://doi.org/10.1038/s41598-020-61168-y

Slatkin, M. (1984). Ecological causes of sexual dimorphism. *Evolution*, *38*(3), 622–630. https://doi.org/10.2307/2408711

Teodecki, E. E., Brodie, E. D., Formanowicz, D. R., & Nussbaum, R. A. (1998). Head dimorphism and burrowing speed in the African caecilian *Schistometopum thomense* (Amphibia: Gymnophiona). *Herpetologica*, *54*(2), 154–160.

Uetz, P., Freed, P., & Hošek, J. (2020). *The reptile database*. http://www.reptile-database.org

Underwood, G. (1967). *A contribution to the classification of snakes*. British Museum (Natural History).

Vincent, S. E., Herrel, A., & Irschick, D. J. (2004). Ontogeny of intersexual head shape and prey selection in the pitviper *Agkistrodon piscivorus*. *Biological Journal of the Linnean Society*, *81*, 151–159. https://doi.org/10.1111/j.1095-8312.2004.00282.x

Wall, F. (1919). Notes on a collection of Snakes made in the Nilgiri Hills and the adjacent Wynaad. *Journal of the Bombay Natural History Society*, *26*, 552–584.

Wall, F. (1921). *Ophidia taprobanica; or, the snakes of Ceylon*. H.R. Cottle, govt. printer.

Watanabe, A., Fabre, A.-C., Felice, R. N., Maisano, J. A., Müller, J., Herrel, A., & Goswami, A. (2019). Ecomorphological diversification in squamates from conserved pattern of cranial integration. *Proceedings of the National Academy of Sciences of the United States of America*, *116*(29), 14688. https://doi.org/10.1073/pnas.1820967116

Zelditch, M. L., Swiderski, D. L., Sheets, H. D., & Fink, W. L. (2004). *Geometric Morphometrics for biologists*. Academic Press.

SUPPORTING INFORMATION

Additional supporting information may be found online in the Supporting Information section.

Figure S1. Tomographic images of the bony tail-shield of *Rhinophis philippinus* specimen BMNH 1964.1701, shown in ventral (a), dorsal (b), lateral (c) and anterior (d) views.

Figure S2. Regression plot of cranial $\log_{10}$-transformed centroid size against a regression score of cranial shape in *Rhinophis philippinus*.

Figure S3. Regression plot of bony tail-shield $\log_{10}$-transformed centroid size against a regression score of tail shield shape in *Rhinophis philippinus*.

Figure S4. Crania of *Rhinophis philippinus* with the minimum (yellow) and maximum (red) values for the PC1 axis displayed in dorsal (a, d), ventral (b, e) and lateral (c, f) views.

Figure S5. Crania of *Rhinophis philippinus* with the minimum (yellow) and maximum (red) values for the PC2 axis displayed in both dorsal (a, d), ventral (b, e) and lateral (c, f) views.

Figure S6. Morphospace of adjusted cranial shape in *Rhinophis philippinus* constructed from PC1 and PC3 axes.

Figure S7. Crania of *Rhinophis philippinus* with the minimum (yellow) and maximum (red) values for the PC3 axis displayed in both dorsal (a, d), ventral (b, e) and lateral (c, f) views.

Figure S8. Bony tail-shields of *Rhinophis philippinus* with the minimum (yellow) and maximum (red) values for the PC1 axis displayed in dorsal (a, d), ventral (b, e) and lateral (c, f) views.

Figure S9. Bony tail-shields of *Rhinophis philippinus* with the minimum (yellow) and maximum (red) values for the PC2 axis displayed in both dorsal (a, d), ventral (b, e) and lateral (c, f) views.

Figure S10. Morphospace of adjusted bony tail-shield shape in Rhinophis philippinus constructed from PC1 and PC3 axes.

Figure S11. Bony tail-shields of *Rhinophis philippinus* with the minimum (yellow) and maximum (red) values for the PC3 axis displayed in both dorsal (a, d), ventral (b, e) and lateral (c, f) views.

Table S1. Descriptions of landmarks applied to crania.

Table S2. Descriptions of curve semilandmarks applied to crania.

Table S3. Descriptions of landmarks applied to bony tail-shield (including fused vertebral elements).

Table S4. Percentage of the variation explained by each principal component for cranial shape of *Rhinophis philippinus*.

Table S5. Percentage of the variation explained by each principal component for tail-shield shape of *Rhinophis philippinus*.

How to cite this article: Huntley, L. C., Gower D. J., Sampaio F. L., Collins E. S., Goswami A., & Fabre A.-C. (2021). Intraspecific morphological variation in the shieldtail snake *Rhinophis philippinus* (Serpentes: Uropeltidae), with particular reference to tail-shield and cranial 3D geometric morphometrics. *Journal of Zoological Systematics and Evolutionary Research*, 00, 1–14. https://doi.org/10.1111/jzs.12505